

Dear Editor,

Thank you for handling this manuscript. We addressed the technical corrections you suggested and we believe that the manuscript is now acceptable for publication.

Sincerely,

Victoria Meyer, on behalf of all co-authors.

Technical corrections bg-2017-547

Abstract:

L 45: Please add a space between “1” and “ha”

A space was added.

Introduction:

L. 89: Should be “e.g.”

“eg.” was replaced by “e.g.”

Material and Methods:

L. 117: Please insert a space between “2000” and “mm”

L. 146 and 154: Please add a space between “1” and “m”

L. 164: Please insert space between “LCA” and “(h)”

L. 165/166: Please add space between number and unit (3 times)

L. 198: Please add space between number and percentage

Spaces were added L.117, 146, 154, 164, 165, 166, 198

L. 137: Delete comma after “Fearnside”

The comma was deleted.

Results:

L. 216: Please indicate a space between number and unit

L. 240 L. 165/166: Please add space between number and unit (2 times)

L. 244: Please add space between number and unit (2 times)

L. 283: Please indicate a space between number and unit

L. 284: Add a space before and after “=”

L. 287: Add a space before and after “=”

Spaces were added L.216, 240, 244, 283, 284, 287

L. 260: The abbreviation for Wood density WD should be either consistently used in the manuscript or avoided. Alternatively many studies use “ρ” to indicate wood density (as you did in the supplements), however it should be clearly defined in the text.

The abbreviation WD is now consistently used throughout the manuscript and supplement.

Discussion:

L. 313: Should be “e.g.”

“eg” was replaced by “e.g.”

L. 322 and 464: Add a comma after et al.

Commas were added.

L. 330: Sometime spaces are indicated after “>” or before “%”, in other cases not, please use constantly the same format.

Spaces were consistently added before “>” and “%” throughout the manuscript, figures and supplement.

L. 362 and 367: Please indicate a space between number and unit

Spaces were added.

References:

L. 80c “, 2010.”?

“, 2010” was removed.

Tables and Figures:

Legend of Table 1: Indicates with uppercase letter. Please format the references in the legend and indicate the significance of “WD” and “AGB” in the legend or below the table as the reader can interpret the results without consulting the text of the manuscript. If you indicate “annual rainfall” there is no need to indicate “yr-1”.

“Indicates” now has uppercase letter. The references were formatted. The significance of WD and AGB were added in the legend. “yr-1” was removed.

Table 1: It would be helpful to indicate the source of rainfall data. Is the annual rainfall in Chocó really 10 meters. I know it rains a lot in this region, but is it such high?

The source of the rainfall data (WorldClim) was added and the reference added to the references list. We based our Choco rainfall number on available literature, but it is now matching the WorldClim data in the specific area we are studying. Chocó rainfall is now 6000mm.

Legend of Table 3: Indicate (WD) after wood density in the legend

“(WD)” was added.

Legend of Figure 4: Shouldn’t it be average wood density (WD)?

The sentence was corrected.

Legend of Figure 5: Please add space between number and unit

A space was added

Supplement:

Legend of Figure S2: Please indicate “height” in lowercase letter

“height is now in lowercase letter.

L. 18: The reference should be Feldpausch. Delete comma after “2013”

The name of the author was corrected and a comma was added.

L. 34 and 126: Please indicate the “-” symbol after cm as subscripted symbol

“-” is now a subscripted symbol.

Table S1: I suggest to indicate the value of RMSE for Antimary also with two decimals

Decimals (0) were added.

Table S3: Also here I suggest to indicate two decimals for the values -0.3 (Bias) 0.8 (R2)

Decimals (0) were added.

Legend of Figure S4: Please insert a space between “1” and “ha” (L. 85)

Legend of Table S4: Please insert a space between “trees” and “ ≥ 50 ” (L. 85)

Spaces were added to Figure S4 and Table S4.

Figure S5: This figure should be improved as the titles of the x- and y-axes are difficult to read

x- and y- axes labels were made bigger.

The listed references should be formatted following the guidelines of Biogeosciences

Please correct:

Chave et al. 2005; Correct the coauthor’s last names (Riéra, Yamakura), substitute the comma after the title by a dot.

Zanne et al. 2009 Please indicate title of the journal, volume and pages

References were corrected and formatted. There is no journal, volume and pages for the Zanne et al. reference.

Additional changes:

The affiliation of one of the co-authors has changed: Fernando Espírito-Santo,
School of Geography, Geology and the Environment, University of Leicester, Leicester LE1 7RH, UK

1 Canopy Area of Large Trees Explains Aboveground
2 Biomass Variations across Neotropical Forest
3 Landscapes
4
5
6

Deleted: Nine

7 Victoria Meyer^{1,2}, Sassan Saatchi¹, David B. Clark³, Michael Keller^{4,5}, Grégoire Vincent⁶, António
8 Ferraz¹, Fernando Espírito-Santo⁷, Marcus V.N. d'Oliveira⁵, Dahlia Kaki¹ and Jérôme Chave²
9

Deleted: ¹,

10 ¹ Jet Propulsion Laboratory, California Institute of Technology, Pasadena, CA, USA
11 ² Laboratoire Evolution et Diversité Biologique UMR 5174, CNRS Université Paul Sabatier, Toulouse,
12 France
13 ³ Department of Biology, University of Missouri, St. Louis, Missouri, U.S.A.
14 ⁴ USDA Forest Service, International Institute of Tropical Forestry, San Juan, Puerto Rico
15 ⁵ EMBRAPA Acre, Rio Branco, Brazil
16 ⁶ IRD, UMR AMAP, Montpellier, 34000 France
17 ⁷ School of Geography, Geology and the Environment, University of Leicester, Leicester LE1 7RH, UK,
18
19
20

Formatted: Font:Times New Roman, Italic
Deleted: Lancaster Environmental Centre, Lancaster University, Lancaster, United Kingdom, LA1 4YQ
Formatted: Line spacing: single
Formatted: Font:(Default) Calibri, Not Italic

21 Correspondence to:

22 Victoria Meyer
23 Jet Propulsion Laboratory
24 California Institute of Technology
25 4800 Oak Grove Drive
26 Pasadena, CA. 91109 USA
27 Email: victoria.meyer@jpl.nasa.com
28
29
30
31
32
33
34
35

40 Abstract

41 Large tropical trees store significant amounts of carbon in woody components and their
42 distribution plays an important role in forest carbon stocks and dynamics. Here, we explore the
43 properties of a new [Lidar](#) derived index, large tree canopy area (LCA) defined as the area
44 occupied by canopy above a reference height. We hypothesize that this simple measure of forest
45 structure representing the crown area of large canopy trees could consistently explain the
46 landscape variations of forest volume and aboveground biomass (AGB) across a range of climate
47 and edaphic conditions. To test this hypothesis, we assembled a unique dataset of high-resolution
48 airborne Light Detection and Ranging ([Lidar](#)) and ground inventory data in nine undisturbed old
49 growth Neotropical forests, [of which four had plots large enough \(1 ha\) to calibrate our model](#).
50 We found that the LCA for trees greater than 27 m (~25–30 m) in height and at least 100 m²
51 crown size in a unit area (1 ha), explains more than 75 % of total forest volume variations,
52 irrespective of the forest biogeographic conditions. When weighted by average wood density of
53 the stand, LCA can be used as an unbiased estimator of AGB [across sites](#) ($R^2 = 0.78$, RMSE =
54 46.02 Mg ha⁻¹, bias = [-0.63](#) Mg ha⁻¹). Unlike other [Lidar](#) derived metrics with complex nonlinear
55 relations to biomass, the relationship between LCA and AGB is linear [and remains unique across](#)
56 [forest types](#). A comparison with tree inventories across the study sites indicates that LCA
57 correlates best with the crown area (or basal area) of trees with diameter [greater than](#) 50 cm. The
58 spatial invariance of the LCA–AGB relationship across the Neotropics suggests a remarkable
59 regularity of forest structure across the landscape and a new technique for systematic monitoring
60 of large trees for their contribution to AGB and changes associated with selective logging, tree
61 mortality, and other types of [tropical](#) forest disturbance and dynamics.

63 **Keywords**

64 [Lidar](#), biomass, tropical forest, large trees, crown area, wood density

65

66 **1 Introduction**

67 In humid tropical forests, tree canopies contribute disproportionately to the exchange of water
68 and carbon with the atmosphere through photosynthesis (Goldstein et al., 1998; Santiago et al.,
69 2004). From a physical standpoint, canopies are rough interfaces formed by crowns of emergent
70 and large trees, regularly disturbed by wind thrusts and gap dynamics. This structurally complex
71 boundary layer is challenging for scaling of biogeochemical fluxes and modeling of vegetation
72 dynamics (Baldocchi et al., 2003). Large canopy trees are among the first to be impacted by
73 storms or heavy precipitation (Espírito-Santo et al., 2010), drought stress (Nepstad et al., 2007;
74 Saatchi et al., 2013; Phillips et al., 2009), and fragmentation (Laurance et al., 2000), potentially
75 leading to tree death and formation of large canopy gaps (Denslow, 1980; Espírito-Santo et al.,
76 2014). Several studies suggest that forest canopies can show fractal properties that tend to evolve
77 from a non-equilibrium state towards a self-organized critical state, involving gap formation and
78 recovery (Pascual and Guichard, 2005; Solé and Manrubia, 1995), with crowns preferentially
79 growing towards more sunlit parts of the canopy (Strigul et al., 2008).

80 Over the past decade, stand level canopy metrics have been increasingly derived using small
81 footprint airborne [Lidar](#) systems (ALS), a widely used remote sensing technique to study the
82 structure of forests (Kellner and Asner, 2009; Lefsky et al., 2002). [Lidar](#) derived mean [top](#)
83 canopy height (MCH) is a good predictor of tropical forest aboveground carbon content and its
84 spatial variability (Jubanski et al., 2013), but it does not provide information on the presence of
85 large trees that are important when monitoring changes of forest biomass from logging and [other](#)

86 small_scale disturbance (Bastin et al., 2015). Moreover, different forests with the same MCH
87 may differ in their stem density, notably of large trees, and in stand mean wood density, two
88 aspects that are important in constructing a robust model to infer AGB from [Lidar](#) data (Asner et
89 al., 2012; Mascaro et al., 2011). Ground observations suggest that stem density, basal area,
90 height and crown size of large tropical trees may all be good indicators of forest AGB (Clark and
91 Clark, 1996; Goodman et al., 2014). This implies that including information on crown area of
92 individual large trees should improve carbon stock assessments, as confirmed in temperate and
93 boreal regions (e.g. Packalen et al., 2015; Popescu et al., 2003; Vauhkonen et al., 2011, 2014).
94 In tropical forests, identifying and delineating crowns of large trees is a difficult and time
95 consuming process due to the layered structure of the forest canopy and overlapping crowns
96 (Zhou et al., 2010, but see Ferraz et al., 2016).
97 Here, we explore how the fractional area occupied by crowns of large trees in a forest stand can
98 be used as a reliable indicator of forest biomass across a wide range of forest structure, climate
99 and edaphic geographic variations. We define large tree canopy area (LCA) as a metric
100 capturing the cluster of crowns of large trees within a forest patch using height and crown area
101 measured by high resolution airborne [Lidar](#) measurements. Precisely, LCA is the number of
102 pixels in the canopy height model above a reference height, and excluding the pixel clusters
103 smaller than a reference area. Since this metric quantifies the proportional presence of large
104 trees, it can be used to estimate AGB and monitor changes associated with the disturbance of
105 large trees from mortality events and selective logging. We first explore the properties of LCA
106 across a range of landscapes in the Neotropics. Next, we hypothesize that LCA is a good
107 predictive metric of the spatial variations of AGB over a wide range of old growth forests.

108 To this end, we assembled a collection of airborne [Lidar](#) measurements and ground inventory
109 data at nine sites in old growth Neotropical forests. The [Lidar](#) data provide variations in canopy
110 height and distribution of large trees that allow us to address the following questions: 1) is there
111 a [single](#) definition of LCA at the landscape scale across different sites? 2) does LCA metric
112 capture variations of AGB?

113

114 **2 Materials and Methods**

115 **2.1 Study sites**

116 We studied the canopy structure at nine old growth lowland Neotropical forest sites that span a
117 broad range of climatic and edaphic conditions (Fig. S1, Table 1). All sites are located in low
118 elevation areas (less than 500 m above sea level) but have small scale surface topography that
119 may influence the distribution of crown formations and gaps. These forests are for the most part
120 undisturbed *terra firme* forests. Tapajós, Antimary and Cotriguaçu get the least rainfall, with
121 approximately 2000 mm yr⁻¹, while La Selva and Chocó both receive more than 4000 mm yr⁻¹
122 (Table 1).

123 Permanent forest inventory plots were available for all sites except Cotriguaçu (Table 1). Sites
124 where tree level inventory data were available were used to estimate the stand level aboveground
125 biomass, thereafter referred to as AGB_{inv}. BCI (50 plots of 1 ha each), Chocó (42 plots of 0.25 ha
126 each), La Selva (11 plots of 1 ha each), Manaus (10 plots of 0.25 ha each), Nouragues (7 plots of
127 1 ha each) and Tapajós (10 plots of 0.25 ha each). In these plots, all trees with a diameter at
128 breast height (DBH) ≥ 10 cm have been mapped, measured and identified to the species. Trees
129 with irregularities or buttresses were measured higher on the bole. Total tree height
130 measurements were available for a subset of these trees. The method for calculating AGB_{inv} from

131 forest inventories is reported in S.1 of the supplementary information. Four sites (BCI, La Selva,
132 Nouragues and Paracou) with 1 ha inventory plots, were used as “calibration sites” to compare
133 the LCA metric and AGB. Sites with smaller plots were not used as calibration of LCA because
134 of the probability of crowns of large trees extending outside the plot boundary and the
135 introduction of uncertainty in estimating LCA from edge effects (Meyer et al., 2013; Packalen et
136 al., 2015). For this reason, all plots smaller than 1 ha were excluded from the LCA analysis but
137 were used in estimating average wood density (WD) for each site, which does not depend on plot
138 size. Stand averaged WD was calculated based on the wood density of all trees present in a site,
139 determined using the commonly used global wood density database, and is reported in Table 1
140 (Chave et al., 2009; Zanne et al., 2009). For Cotriguaçu, we used stand averaged WD given by
141 Fearnside (1997) for a region covering the site. Additional plot level data (AGB_{inv} and mean
142 WD) were provided for Antimary (50 plots of 0.25 ha each), Nouragues (27 plots of 1 ha each)
143 and Paracou (85 plots of 1 ha each).

Deleted: wood density

Deleted: wood density

145 2.2 Lidar data

146 Lidar sensors scan the vegetation vertical structure and return a three dimensional point cloud
147 derived from the time it took each pulse to return to the instrument. The Lidar datasets acquired
148 over the study sites come from discrete return Lidar instruments and were gridded horizontally at
149 a 1_m resolution using the echoes classified as either vegetation or ground. They yield three
150 products: digital surface model (DSM) corresponding to the top canopy elevation, digital terrain
151 model (DTM) corresponding to the ground elevation, and canopy height model (CHM), which is
152 the height difference between the DSM and the DTM. DTMs were interpolated from a Delaunay
153 triangulation or comparable interpolation methods, after outliers have been removed. DSMs were

created using the highest return within a cell. [Lidar](#) data over Paracou were acquired in last return mode, causing a bias of 50 cm on the CHM (Vincent et al., 2012). This bias is not addressed in this study because our height increment for the determination of optimal height thresholding is larger (1_m) (see Sect. 4.3). Data were acquired between 2009 and 2013, using relatively similar sensors and acquisition configurations (Table 2). The potential differences between the [Lidar](#) datasets and their impact on the results are addressed in the Discussion. For each site, we selected a 1x1 km (100 ha) area of old growth forest, oriented north-south, without any human disturbance to the extent possible. Topography derived from [Lidar](#) data within the selected 1 km² subset images provides information on landscape variations that may impact the forest structure. Data visualization was done using ENVI version 4.8 (Exelis).

2.3 Computing Large Canopy Area (LCA)

At each study site, we extracted the area of canopy that relates to total area of the canopy height model above a standard height (h) threshold, or LCA_h, and explored how this metric scales along two axes. First, we varied the threshold height h with increments of 1_m, between 5_m and 50_m, in 100 m by 100 m subareas (100 subareas for each site). Second, to denoise the data, we excluded the clusters with less than a set number of 1m² pixels (50, 100, 150 or 200). We then prioritized the crown area of large trees, and filtered out pixels that could be related to outliers or to single branches. This method thus quantifies the area of large crowns covering a plot or larger landscape unit area, as a percentage of covered area.

LCA maps were produced at 1 ha resolution. Pixel clustering was based on the similarity of the four nearest neighbors (similar results were obtained with an eight_neighbor model, results not shown here). Figure S2 summarizes the steps taken to go from the [Lidar](#) canopy height model to

179 the final LCA map. Processing was conducted using the IDL software (Interface Description
180 Language, Exelis).

181 We determined the optimal minimum canopy height threshold calculating the coefficient of
182 correlation between AGB_{inv} and LCA at the four calibration sites. This step allowed us to
183 examine if optimal height thresholds differed from one site to the other. The goal was to find a
184 single optimal height threshold and crown size that could be applied for LCA retrieval across
185 closed canopy Neotropical forests. We also estimated AGB from Lidar data locally (AGB_{Local})
186 using a commonly used model fit relating MCH to AGB_{inv} in each site, to further examine the
187 variations of LCA and AGB in all nine sites (see S.2, Table S1).

189 2.4 Relating LCA to biomass

190 We tested different models to infer AGB_{inv} from LCA, henceforth called AGB_{LCA}, at the four
191 calibration sites, and explored if adding more parameters, such as mean ~~WD~~ of a site, mean ~~WD~~
192 of large trees (DBH \geq 50 cm), mean canopy height or top percentiles of canopy height improved
193 the predicting power of the model. We evaluated our results by applying a jackknife validation to
194 our regression models, based on 1000 iterations of bootstrapping. The coefficients of correlation
195 (R²), root mean square error (RMSE) and bias (mean difference between the expected values of
196 AGB and the observed values of AGB) are reported for the models providing the best results.
197 The analysis was performed using the R statistical software (R Core Team, 2014).
198 We compared the new approach based on LCA to a similar approach based on MCH, which
199 relies on information on all pixels of an area of interest. In both cases, models were calibrated by
200 using field data from the four calibration sites and their respective mean WD. This comparison is

Deleted: wood density

Deleted: wood density

meant to investigate if a metric based on large trees only (LCA) can estimate AGB similarly to a metric that uses information about 100 % of the canopy (MCH).

2.5 Detecting changes of selecting logging

Forest degradation due to selective logging is difficult to detect with conventional remote sensing techniques due to small scale and minor impacts on the forest canopy and biomass compared to severe forest disturbances (e.g. fires, storms, or clearing). However, selective logging targets large trees (Pearson et al., 2014) and thus may be detectable using LCA, provided that Lidar data are available from pre and post-logging. Here, we use the Antimary study site that was selectively logged after the 2010 Lidar acquisition to examine the use of LCA for detecting logging impacts on the forest canopy and AGB. We apply the large tree segmentation approach on both the 2010 image and on a 2011 post-logging Lidar image (see Andersen et al., 2014 for details) to quantify the logging impacts in terms of the distribution of large trees removed from the forest and the loss of aboveground biomass.

3 Results

3.1 Intersite comparison of landscapes and MCH

Topographic variation within the 1 km² images ranged from about 4 m elevation gain in flat area of Tapajós to steep elevation gain of up to about 100 m in Cotriguaçu and Chocó (Fig. S3). Top canopy height reached up to 60 m, but varies across sites, with Chocó having the lowest MCH (24.1 m) and Nouragues the highest (29.7 m). Forest height in Manaus was more homogeneous than in the other sites, with a standard deviation of 6.8 m for MCH, versus 10.3 m in Paracou.

225 We found no relationship between topography and canopy height, which suggests that variability
226 in forest structure may be due to other ecological and edaphic factors in each site.

227
228

229 **3.2 Large canopy area index**

230 The choice of the canopy height threshold impacted LCA more than the minimum number of
231 pixels per cluster (Table S2). The difference due to the choice of the minimal cluster size
232 threshold was on average 1.4 %, calculated as the mean of the difference between the smallest
233 grain (50 pixels) and the largest one (200 pixels) across sites and height thresholds. Based on this
234 analysis, we chose to define LCA using a minimum cluster size of 100 pixels (100 m² for crown
235 area) in the remainder of this study. This corresponds to an area of at least 10 m x10 m or a circle
236 of approximately 11m in diameter, consistent with the average crown diameter of large trees of
237 the region (Bohlman and O'Brien, 2006; Figueiredo et al., 2016; Clark, unpublished results).

238
239 In contrast, the canopy height thresholds markedly impacted the magnitude of LCA among sites
240 (Fig. 1 and Fig. 2, Table S2). As the height threshold increased, intra-site variation of LCA(h)
241 became apparent, showing differences of LCA associated with differences of forest structure
242 (Fig. 1). Tapajós and Nouragues stood out with more area of large trees at the height threshold of
243 30 m ($LCA_{30m} = 51$ and 48 %, respectively) , while Antimary and Chocó showed much lower
244 LCA at this height threshold ($LCA_{30m} = 21$ %) (Table S2). The steepest slopes of the LCA(h)
245 function corresponded to the highest sensitivity of LCA to height thresholds and the inflection in
246 LCA was found between 24_m in Antimary and 30_m in Nouragues (Fig. 2). The average height
247 of the steepest slope was about 27 m, a value that was used as the optimal threshold across all
248 sites.

249 Regressing AGB_{inv} and LCA at the calibration sites (Fig. 3b) showed the best relationships
250 corresponded to height thresholds between 27_m (Nouragues and Paracou) and 28_m (BCI and
251 La Selva), with maximum coefficients of correlation ranging between 0.5 and 0.8. The same
252 analysis repeated using AGB_{local} and LCA in the nine sites also confirmed the earlier results that
253 the highest coefficients of correlation between the two metrics occurred between 23 m (Chocó)
254 and 30 m (Tapajós) height thresholds (Fig. 3a), explaining more than 75 % of AGB variation in
255 each site. Based on these results, we defined LCA as the cumulative area of clusters of the
256 canopy height model greater than 27 m height, as the mean of optimal height threshold with
257 highest R² across sites, with clusters covering areas larger than 100 m².

259 3.3 Variation of AGB derived from LCA

261 AGB_{inv} was found to depend linearly on LCA (Eq. 1), with a better coefficient of correlation and
262 RMSE than a power law fit ($R^2_{\text{linear}} = 0.59$, $\text{RMSE}_{\text{linear}} = 62.53 \text{ Mg ha}^{-1}$, vs. $R^2_{\text{power}} = 0.54$,
263 $\text{RMSE}_{\text{power}} = 65.38$). Although this model was unbiased ($\text{bias}_{\text{cross_val}} = 0.16 \text{ Mg}$), there were clear
264 differences among study sites (Fig. 4a, Table 3). These differences were largely explained by
265 landscape scale differences in WD, an important factor representing the influence of species
266 composition on the spatial variation of AGB. Since AGB depends on DBH, H and WD (see
267 Chave et al., 2014), average wood volume can be computed approximately as the ratio of AGB
268 divided by the average WD (Fig. 4b). The linear relationship between LCA and wood volume
269 yielded an estimate of the average total volume of forests independently of the site
270 characteristics, through $\text{Vol} = a \text{ LCA} + b$. Adding more parameters did not improve the

Deleted: wood density

Deleted: wood density

performance of the model, except when using WD as a normalizing factor. The two models we retained are therefore of the form of Eq. (1) and Eq. (2):

$$AGB_{LCA} = a LCA + b \quad (1)$$

$$AGB_{LCA} = (a LCA + b) \times WD \quad (2)$$

where here WD is the mean wood density of a site. The coefficients of the models, as well as their respective coefficients of correlation, RMSE and bias from training data and cross-validation are reported in Table 3.

For AGB estimation, the model based on LCA weighted by WD gives the best result by bringing R^2 up to 0.78 and RMSE down to 46.02 Mg ha⁻¹ (Fig. 4b, Fig. 4c, Table 3, Eq. (2)), with AGB_{inv} and AGB_{LCA} falling around a one-to-one line in Fig. 4c. At all sites, RMSE values are between 20.87 and 42.22 Mg, except Nouragues, where RMSE remains large (71.21 Mg) due to high biomass and several outliers from the linear relation. The relationship between LCA and other metrics derived from ground data, such as Lorey's height or basal area, are presented in S.3 and Table S4.

3.4 LCA vs. MCH approach

Finally, we compared these results to AGB estimated using a similar approach based on MCH (AGB_{MCH}) for the calibration plots (Fig. 5a), and we also compared AGB_{LCA} to AGB_{MCH} in all nine sites, using LCA and MCH of the 1 km² images (Fig. 5b).

Both methods perform similarly ($R^2_{MCH} = 0.80$, $RMSE_{MCH} = 42.52$ Mg ha⁻¹, $bias_{cross_val} = -0.21$ Mg ha⁻¹, Table S3), showing that relying on a fraction of the Lidar information performs as well as using a metric depending on information from all pixels. However, Fig. 5 also shows that the

LCA method tends to overestimate AGB compared to the MCH method (bias = 9.66 Mg ha⁻¹), especially in La Selva, BCI, Cotriguaçu and Manaus.

3.5 AGB changes from logging

The impacts of logging on the distribution of large trees and changes of AGB was detected by simply deriving the LCA index from pre and post-logging Lidar data acquired in 2010 and 2011 respectively in Antimary (Fig. 6). Difference in LCA between the two dates (2010–2011) (Fig. 6a) at 1 ha grid cell captured the areas of largest changes in the few months following logging (logging took place between June and November 2011, Lidar data were collected in late November 2011). The LCA approach was able to detect approximately a 17 % decrease in LCA, from a mean LCA of 34.8 % in 2010 to 29.2 % in 2011.

The changes were also captured in the frequency distribution of large canopy trees before and after logging (Fig. 6b) and the differences in the spatial distribution (Fig. 6c and 6d).

These changes in LCA correspond to a biomass loss of 15.2 Mg ha⁻¹ when integrated in equation (2) and were of the same magnitude of the planned selectively logging removal rate (12–18 Mg ha⁻¹ or 10–15 m³ ha⁻¹ of timber volume) (Andersen et al., 2014). As a comparison, the MCH model led to an estimated biomass loss of 19 Mg ha⁻¹. Difference in the Lidar index (ΔLCA) at the native resolution of 1 m (Fig. 6e) was able to capture both the location of all large trees removed from the forest stand and partial regeneration and gap filling that occurred in the forest between the two dates.

4 Discussion

4.1 Inter-site Comparisons

318 Cross-site studies on the structure of tropical forests have led to significant advances in our
319 understanding of tropical forest ecology (Gentry 1993; Phillips et al., 1998; ter Steege et al.,
320 2006). They have also yielded important insights on new techniques to predict carbon stocks
321 across regions (e.g. Asner and Mascaro, 2014). Comparison of sites in terms of MCH derived
322 for the study sites confirms that there is a strong regional variation of AGB with respect to
323 canopy height, and that East Amazonian sites tend to have much taller trees than Central and
324 Western Amazonia sites. This was already apparent in the canopy height maps produced by the
325 GLAS sensor (Lefsky, 2010; Saatchi et al., 2011; Simard et al., 2011). Comparing sites in terms
326 of LCA showed a similar pattern of larger trees, being relatively more present in eastern
327 Amazonia, notably in the French Guiana sites and Tapajos. Our most southwestern site was
328 Antimary, in the state of Acre (Brazilian Amazon). However, this site does not represent forests
329 in the western Amazon or the Amazon-Andes gradients with relatively lower WD (Baker et al.,
330 2004) and more fertile volcanic soils impacting the forest structure and dynamics (Quesada et al.,
331 2011). The site in Chocó is also unique in its characteristics because of extremely wet condition
332 and potential disturbance (e.g., selective logging). Additional Lidar and ground measurements
333 will allow validating the performance of the LCA in representing the AGB variations in the
334 western Amazon region.

336 4.2 Physical Interpretation of LCA

337 In this study, we introduced a simple structural metric that captures the proportion of area
338 covered by large trees over the landscape (> 1 ha) and explained 78 % of the variation in
339 average forest volume and biomass when weighted by WD in four sites of old growth
340 Neotropical forests. LCA cannot separate the crown areas of individual trees. However, it is

Deleted: wood density

adapted for large scale monitoring of forest volume and biomass change, as it is a robust and readily accessible metric. For individual tree separation, complex and more computationally intensive approaches are available (Ferraz et al., 2016).

In estimating LCA from [Lidar](#) data, we examined the spatial clustering properties of LCA and found that the minimum cluster size was less important than the threshold of canopy height, as long as the analysis focused on the relative covered area instead of on the density of large trees. We found that using the percentage of the area covered by large canopy trees is an efficient way of overcoming the problem of individual crown segmentation in [Lidar](#) data. LCA is related to how trees reaching the forest canopy (above a certain height) fill the space and how this characteristic may follow a spatially invariant scaling across tropical forests (West et al., 2009). Clusters smaller than 100 m² add only a small fraction (1.7 % on average) to LCA values across sites. Including these clusters in LCA would not impact the performance of the model (similar R², RMSE and bias) and would allow to skip the final steps of the LCA retrieval (see Fig. S2). However, since these pixels either represent single branches reaching above 27m or the tip of a tree crown, they have no meaning in terms of our LCA metric and do not represent large trees. LCA provides information on the presence of large trees in a study area, which other metrics such as MCH cannot do. It is an important point, considering that large trees are often the most affected by natural disturbance and targeted by logging companies.

4.3 Correlation between LCA and AGB

The distribution of R² between LCA and AGB for (Fig. 3) is such that the maximum difference in R² between a threshold of 25m and 30m is approximately 0.1, a negligible value. Hence, AGB retrieval by LCA is relatively insensitive to the height threshold. For most sites, except

Antimay, we found a height threshold such that LCA explains about 80–90 % of the variation of AGB or total volume of the forests for each site (60–70 % when compared with ground plots) (Fig. 3). Using a height threshold of 27 m for all sites reduced the R^2 by 0.04 on average (max = 0.08) compared to the optimal height threshold for each site.

Potential differences in MCH among sites are due to footprint size, scan angle and return density (Disney et al., 2010; Hirata, 2004; Hopkinson, 2007) (Table 2). However, these effects are generally smaller than the 1 m increment that we used to determine the optimal height thresholds of LCA. As a result, LCA estimation, and therefore AGB inferred from LCA, should depend little on instrument, acquisition and processing (Table 2). This is an important finding given the increasing variety of airborne Lidar sensors, and also given the pre and post-processing methods available for monitoring tropical forest structure and aboveground biomass. However, determining whether the 27 m threshold holds for LCA calculation across in the tropics would require a validation at more study studies across continents.

4.4 LCA Relation to Ground Measurements

The relation between LCA derived from Lidar and the ground measurements can be further investigated by converting the 27 m height threshold into equivalent DBH values, using a height–diameter relationship. In the absence of a local DBH–height relation at each site, we made use of the following equation (Chave et al., 2014):

$$\ln(H) = 0.893 - E + 0.760 \times \ln(D) - 0.0340 \times (\ln(D))^2 \quad (3)$$

where E is a measure of environmental stress for each site that potentially impacts the tree allometry. The corresponding DBH values fall around 35–55 cm, except for Chocó, where the best coefficient of correlation is reached with a DBH threshold of 29 cm (Fig. S4). The average

minimum DBH to assign for the definition of large trees that represent variations of AGB is
 below 50 cm. By choosing a DBH threshold of 50 cm for old-growth undisturbed forests, the
 LCA model for estimating biomass can have an approximate analog in inventory data. This
 comparison suggests that the LCA model can also be adjusted with the average ~~WD~~ of trees
 larger than 50 m, allowing a much faster ground data collection of calibrating LCA model for
 different sites (S.4).

A limit to how much LCA can explain variations in AGB relates to forest structure and the AGB
 of small trees. The lower range of biomass estimation for the LCA model, associated with the
 intercept for LCA equal to zero, ranged between 122 Mg ha⁻¹ in La Selva and 192 Mg ha⁻¹ in
 Paracou (Fig. 7a). This lower range identified with the intercept of the LCA–AGB linear model
 can be interpreted as the AGB associated with all trees smaller than 27 m height (approximately
 all trees with DBH < 50 cm). Note that the differences between sites are due to differences in
 their mean ~~WD~~ and not the volume of trees (see Eq. (2) and Fig. 4). Similarly, the contribution of
 small trees to the total biomass in the ground inventory ranges between around 100 and 200 Mg
 ha⁻¹, except in Paracou (261 Mg ha⁻¹) (Fig. 7b). AGB estimation based on LCA in these sites
 cannot go under 100 Mg ha⁻¹ or over 500 Mg ha⁻¹. This is not a limitation of the model because
 LCA is designed to provide AGB estimates for forests reaching at least 27 m in mean canopy
 height, and such forests generally exceed 100 Mg ha⁻¹ in AGB. Also, the upper threshold of 500
 Mg ha⁻¹ is consistent with upper values found globally at 1 ha scale (Brienen et al., 2015; Slik et
 al., 2013). A recalibration of the method should be envisaged in secondary and highly degraded
 forests.

Deleted: wood density

Deleted: wood density

413 4.5 LCA as AGB Estimator

414 The correlation of LCA to AGB_{inv} suggests that a Lidar based approach can lead to the
415 estimation of AGB at the landscape scale and give useful information on the presence of large
416 canopy trees and their distribution, extending the analysis of large trees in plot level inventory
417 based studies (Bastin et al., 2015; Slik et al., 2013).

418 Therefore, LCA can explain the variations of total forest volume without any ancillary data about
419 the forest or the landscape. Most bias in conversion of LCA to AGB, however, can be corrected
420 across landscapes and sites by scaling the LCA–AGB relationship with average WD at the
421 landscape scale. Our model can therefore potentially be applied to a wide range of forest types,
422 provided that there is information about WD of the study area in the literature.

423 Wood density has been shown to be a key element of allometric models of AGB estimation
424 (Baker et al., 2004; Brown et al., 1989; Chave et al., 2004; Nogueira et al., 2007). If WD is
425 assumed to be constant across DBH classes, the mean WD at the plot scale can readily be used to
426 scale LCA to biomass. However, if the WD of large trees is smaller or larger than the average
427 WD, (e.g. in BCI and Chocó: S.4, Fig. S5), the use of mean WD to scale LCA may introduce a
428 slight bias in biomass estimation. A difference in mean WD of 0.1 g cm^{-3} would introduce a bias
429 of $\pm 10 \%$ in the biomass estimation when using our model. We found that using mean WD of
430 large trees or basal area weighted WD instead can give slightly better results and could
431 circumvent the differences in size distribution of the WD (S.4). Instead we could rely on the
432 WD of large trees only. This would make the collection of ground data easier and cost effective
433 for biomass estimation, because trees ≥ 50 cm DBH only represent 5–10 % of the stems of a plot
434 (S.4, Fig. S6). Focusing on the WD of dominant or hyper dominant species could also be an
435 alternative approach for future use of Lidar derived LCA for large scale biomass estimation

Deleted: wood density

Deleted: Wood density

Deleted: wood density

Deleted: wood density

Deleted: wood density

Deleted: wood density

Deleted: wood density

Deleted: wood density

Deleted: wood density

Deleted: wood density

Deleted: wood density

Deleted: wood density

Deleted: wood density

(Fauset et al., 2015; ter Steege et al., 2013). In the absence of information on WD from the literature, modelled WD could potentially be used, but would give greater errors. These errors should be taken into account when reporting on the uncertainty of the results.

4.6 LCA and MCH

The comparison of LCA and MCH metrics showed that both performed similarly in estimating AGB, highlighting the importance of large canopy trees to estimate biomass. The differences between the two methods in estimating AGB show that two methods can have similar performance in terms of R^2 and RMSE and nonetheless lead to different estimations, with LCA giving higher AGB estimations in some sites. The choice of a metric is therefore crucial to estimate AGB, especially when estimating the changes in biomass (see Section 4.7).

Both MCH and LCA–AGB models performed relatively poorly in high biomass plots of the Nouragues study area, by underestimating biomass values greater than 500 Mg ha⁻¹ (Fig. 4 and 5). To explain the underestimation, we performed three tests: 1. We examined the differences in the ground estimated biomass values with and without tree height and found no significant impact in reducing the effect of underestimation. 2. We tested the hypothesis that the height threshold used for LCA estimation across sites was not suitable for the Nouragues study site and dismissed the hypothesis because 27 m was found to be the optimum threshold for Nouragues plots. 3. We examined the errors in the Lidar estimation of forest height and found that except for an extremely high AGB_{inv} of 617 Mg ha⁻¹, the four other high biomass outliers are all located in the 6 ha Pararé plot located on a very steep topography. The Lidar digital terrain model (DTM) of this area shows an average within plots elevation range of 90 m. Ground detection on steep terrain can be erroneous, depending on the Lidar point density and the view angle, causing

large area interpolation errors for DTM development and significant error in canopy height measurements (Leitold et al., 2015). Other factors that may affect the underestimation of AGB by LCA or MCH in the Nouragues site may be due to the presence of forest patches with clusters of large trees and overlapping crown areas. It is also possible that the relationship between AGB and LCA is not linear for very high AGB values. This could be tested in the future with a larger number of sites with very high biomass.

4.7 LCA and forest degradation

Although LCA and MCH may perform similarly in capturing the forest biomass variations and changes, the use of LCA in detecting forest degradation and logging is more straightforward because of its relation to large trees. The LCA approach was able to accurately detect changes in forests after logging by locating where the large trees are extracted. Our estimate of biomass change from the LCA approach was higher than the biomass loss of 9.1 Mg ha⁻¹ reported by another study using the 25th percentile height above ground as the Lidar metric for biomass estimation (Andersen et al., 2014). It can be expected that relying on the 25th percentile height metric for biomass estimation would place more emphasis on the lower part of the canopy (understory) that is either less damaged or has gone through some level of regeneration after logging. Models based on LCA or MCH, on the other hand, may be more realistic for estimating AGB changes because they capture the changes in large trees and upper forest canopy structure that contain most of the biomass and are directly impacted by logging and biomass removal. The higher biomass loss estimation from the MCH model (19 Mg ha⁻¹) again shows how different metrics can lead to different results. Here, three methods based on three different Lidar metrics yielded results that differed by more than twofold. LCA could become an important tool

to detect forest degradation, in particular selective logging, considering that large trees are targeted by logging companies.

4.8 Future Applications of LCA

LCA definition in our study relies on the high-resolution information on forest height, allowing for the detection of crown area of large canopy trees. Can a similar measure be derived from large footprint Lidar observations such as the future NASA spaceborne Lidar mission GEDI (Global Ecosystem Dynamic Investigation)? GEDI will not provide spatially continuous data on forest height, but its footprint size (~ 25 m) and dense sampling may be adequate to develop statistical indicators of large trees over the landscape.

Similarly, future spaceborne radar missions could also provide useful information to retrieve large canopy areas. The synthetic aperture radar (SAR) tomographical observations of the European Space Agency (ESA) BIOMASS mission will provide wall-to-wall imagery of canopy profile that could be converted to LCA over the landscape (Le Toan et al., 2011). Preliminary research based on airborne TomoSAR measurements has already shown that backscatter power at about 30 m above the ground, with sensitivity to the distribution of large trees, explained the variation of AGB over Nouragues and Paracou plots better than the backscatter power related to the lower part of the canopy (0–15 m) (Minh et al., 2016; Rocca et al., 2014). Future research on exploring the use of an equivalent radar index product from BIOMASS height or tomography measurements at a height threshold (e.g. 27 m) may provide a potential algorithm to map the area of large trees and estimate forest volume and biomass changes across the landscape.

518 5 Conclusions

519 We introduce LCA as a new [Lidar](#) derived index to capture the variations of large trees and total
520 volume and biomass across landscapes that remain spatially and regionally invariant. The
521 importance of LCA is in its relevance to the structure and ecological characteristics of large trees
522 in filling the canopy space and their unique contribution in determining the total volume and
523 biomass of forests. Unlike other [Lidar](#) derived metrics, LCA is linearly related to total
524 aboveground biomass after being weighted by average [WD](#). [This linear relationship remains](#)
525 [unique across different forest types, making the LCA model broadly applicable.](#) The comparison
526 of LCA index with ground plots suggests that DBH > 50 cm is a more reliable threshold to
527 quantify the number and distribution of large trees [in undisturbed old growth tropical forests](#) and
528 in capturing the variations of the total aboveground biomass across landscapes and regions. [The](#)
529 [results of our study may encourage further research in the use of Lidar data for detecting the](#)
530 [distribution of larger trees in tropical forests for ecological and conservation studies.](#)

Deleted: wood density

533 Author contribution

534 V. Meyer and S. Saatchi developed the model and designed the study. V. Meyer developed the
535 model code and performed the analysis. J. Chave, G. Vincent, M. Keller, F. Espirito-Santo, D.
536 Clark and M. d'Oliveira provided inventory data and derived metrics necessary to run the
537 experiments. A. Ferraz contributed to the data processing. D. Kaki performed a preliminary
538 analysis of the data. V. Meyer prepared the manuscript with contributions from all co-authors.
539 The authors declare that they have no conflict of interest.

540

542 Acknowledgements

543 The work described in this paper was carried out at the Jet Propulsion Laboratory, California
544 Institute of Technology, under contract with the National Aeronautics and Space Administration.
545 This work has benefited from “*Investissement d’Avenir*” grants managed by the French *Agence*
546 *Nationale de la Recherche* (CEBA, ref. ANR-10-LABX-25-01 and TULIP, ref. ANR-10-LABX-
547 0041; ANAEE-France: ANR-11-INBS-0001) and from CNES (TOSCA project; PI T Le Toan).
548 Field and [Lidar](#) data from the Brazilian sites were acquired by the Sustainable Landscapes Brazil
549 project supported by the Brazilian Agricultural Research Corporation (EMBRAPA), the US
550 Forest Service, and USAID, and the US Department of State. La Selva field work was supported
551 by the U.S. National Science Foundation LTREB Program NSF LTREB 1357177. Data in Chocó
552 are available as part of the Reducing Emissions from Deforestation and forest Degradation
553 (REDD) project. FES was supported by Natural Environment Research Council (NERC) grants
554 (‘BIO-RED’ NE/N012542/1 and ‘AFIRE’ NE/P004512/1) and Newton Fund (‘The UK
555 Academies/FAPESP Proc. N°: 2015/50392-8 Fellowship and Research Mobility’). The AGB
556 data for Paracou were made available courtesy of CIRAD (B. Hérault).

557
558 © 2018. All rights reserved.

Deleted: 7

562 Data accessibility

563 The BCI [Lidar](#) and forest inventory dataset used in this research are publically available from the
564 Office of Bioinformatics, Smithsonian Tropical Research Institute. All relevant data are within
565 the paper and its Supporting Information files.

568 References

- 569
570 Andersen, H. E., Reutebuch, S. E., McGaughey, R. J., d'Oliveira, M. V. and Keller, M.:
571 Monitoring selective logging in western Amazonia with repeat [lidar](#) flights. *Remote Sens.*
572 *Environ.*, 151, 157-165, 2014.
573
574 Asner, G. P., Mascaro, J., Muller-Landau, H. C., Vieilledent, G., Vaudry, R., Rasamoelina, M.,
575 Hall, J. S. and van Breugel, M.: A universal airborne [Lidar](#) approach for tropical forest carbon
576 mapping. *Oecologia*, 168(4), 1147-1160, 2012.
577
578 Asner, G. P. and Mascaro, J.: Mapping tropical forest carbon: Calibrating plot estimates to a simple
579 [Lidar](#) metric. *Remote Sens. Environ.* 140, 614-624, 2014.
580
581 Baker, T. R., Phillips, O. L., Malhi, Y., Almeida, S., Arroyo, L., Di Fiore, A., Erwin, T., Killeen,
582 T. J., Laurance, S. G., Laurance, W. F. and Lewis, S. L.: Variation in wood density determines

584 spatial patterns in Amazonian forest biomass. *Glob. Change Biol.*, 10(5), 545-562. doi:
585 10.1111/j.1365-2486.2004.00751.x, 2004.

586

587 Baldocchi, D. D.: Assessing the eddy covariance technique for evaluating carbon dioxide exchange
588 rates of ecosystems: past, present and future. *Glob. Change Biol.*, 9(4), 479-492, 2003.

589

590 Basset, Y., Cizek, L., Cuénoud, P., Didham, R. K., Guilhaumon, F., Missa, O., Novotny, V.,
591 Ødegaard, F., Roslin, T., Schmidl, J. and Tishechkin, A. K.: Arthropod diversity in a tropical
592 forest. *Science*, 338(6113), 1481-1484, 2012.

593

594 Bastin, J.-F., Barbier, N., Réjou-Méchain, M., Fayolle, A., Gourlet-Fleury, S., Maniatis, D., de
595 Haulleville, T., Baya, F., Beeckman, H., Beina, D. and Couteron, P.: Seeing Central African forests
596 through their largest trees. *Sci. Rep.-UK*, 5, 13156, 2015.

597

598 Bioredd.org/ accessed 4.13.2016

599

600 Bohlman, S., and O'Brien, S.: Allometry, adult stature and regeneration requirement of 65 tree
601 species on Barro Colorado Island, Panama. *J. Trop. Ecol.*, 22(02), 123-136, 2006.

602

603 Brien, R. J. W., Phillips, O. L., Feldpausch T. R., Gloor E., Baker, T. R., Lloyd, J. and Lopez-
604 Gonzalez G.: Long-Term Decline of the Amazon Carbon Sink. *Nature*, 519, 344.
605 <http://dx.doi.org/10.1038/nature14283>, 2015.

606

607 Brown, S., Gillespie, A. J., and Lugo, A. E.: Biomass estimation methods for tropical forests with
608 applications to forest inventory data. *Forest Sci.*, 35(4), 881-902, 1989.

609

610 Chave, J., Condit, R., Aguilar, S., Hernandez, A., Lao, S., and Perez, R.: Error propagation and
611 scaling for tropical forest biomass estimates, *Philos. T. R. Soc. B*, 359, 409–420, 2004.

612

613 Chave, J., Réjou-Méchain, M., Búrquez, A., Chidumayo, E., Colgan, M. S., Delitti, W. B., and
614 Vieilledent, G.: Improved allometric models to estimate the aboveground biomass of tropical trees.
615 *Glob. Change Biol.*, 20(10), 3177-3190, 2014.

616

617 Clark D. B. and Clark D. A.: Abundance, growth and mortality of very large trees in neotropical
618 lowland rain forest. *Forest Ecol. and Manag.*, 80, 235–244, 1996.

619

620 Clark, D. B. and Clark, D. A.: Landscape-scale variation in forest structure and biomass in a
621 tropical rain forest. *Forest Ecol. and Manag.*, 137, 185–198, 2000.

622

623 Condit, R.: *Tropical Forest Census Plots*. Springer Verlag and R.G. Landes Company. Berlin and
624 Georgetown, TX, 1998.

625

626 d'Oliveira, M. V. N., Reutebuch, S. E., McGaughey, R. J. and Andersen, H. E. : Estimating
627 forest biomass and identifying low-intensity logging areas using airborne scanning [lidar](#) in
628 Antimary State Forest, Acre State, Western Brazilian Amazon. *Remote Sens. Environ.*, 124, 479-
629 491, 2012.

630
631 Denslow, J. S. : Gap portioning among tropical rainforest trees. *Biotropica*, 12, 47–55, 1980.
632
633 Disney, M. I., Kalogirou, V., Lewis, P., Prieto-Blanco, A., Hancock, S., and Pfeifer, M.:
634 Simulating the impact of discrete-return [Lidar](#) system and survey characteristics over young
635 conifer and broadleaf forests. *Remote Sens. Environ.*, 114(7), 1546-1560, 2010.
636
637 ENVI/IDL, Exelis Visual Information Solutions, Boulder, Colorado.
638
639 Espírito-Santo, F. D. B., Keller, M., Braswell, B., Nelson, B. W., Frohking, S., and Vicente, G.:
640 Storm intensity and old-growth forest disturbances in the Amazon region. *Geophys. Res. Lett.*,
641 37(11), 2010.
642
643 Espírito-Santo, F. D. B., Keller, M. M., Linder, E., Oliveira, R. C. Junior, Pereira, C. and
644 Oliveira, C. G.: Gap formation and carbon cycling in the Brazilian Amazon: measurement using
645 high-resolution optical remote sensing and studies in large forest plots. *Plant Ecol. Divers.*, 7,
646 305–318, 2014.
647
648 Fauset, S., Johnson, M. O., Gloor, M., Baker, T. R., Monteagudo, A., Brien, R. J., Feldpausch,
649 T. R., Lopez-Gonzalez, G., Malhi, Y., Ter Steege, H. and Pitman, N. C.: Hyperdominance in
650 Amazonian forest carbon cycling. *Nat. Commun.*, 6, 2015.
651
652 Fearnside, P. M.: Wood density for estimating forest biomass in Brazilian Amazonia. *Forest Ecol.*
653 *and Manag.*, 90(1), 59-87, 1997.
654
655 Ferraz, A., Saatchi, S., Mallet, C., and Meyer, V.: [Lidar](#) detection of individual tree size in tropical
656 forests. *Remote Sens. Environ.*, 183, 318-333, 2016.
657
658 Figueiredo, E. O., d'Oliveira, M. V. N., Braz, E. M., de Almeida Papa, D. and Fearnside, P. M.:
659 [LIDAR](#)-based estimation of bole biomass for precision management of an Amazonian forest:
660 Comparisons of ground-based and remotely sensed estimates. *Remote Sens. Environ.*, 187, 281-
661 293, 2016.
662
663 Gentry, A. H.: Four neotropical rainforests. Yale University Press, 1993.
664
665 Goldstein, G., Andrade, J. L., Meinzer, F. C., Holbrook, N. M., Cavelier, J., Jackson, P., and Celis,
666 A.: Stem water storage and diurnal patterns of water use in tropical forest canopy trees. *Plant Cell*
667 *Environ.*, 21(4), 397-406, 1998.
668
669 Goodman, R. C., Phillips, O. L., and Baker, T. R.: The importance of crown dimensions to improve
670 tropical tree biomass estimates. *Ecol. Appl.*, 24(4), 680-698, 2014.
671
672 Gourlet-Fleury, S., Guehl, J.-M. and Laroussinie, O.: Ecology and management of a neotropical
673 rainforest. Lessons drawn from Paracou, a long-term experimental research site in French
674 Guiana. Elsevier, Amsterdam, 2004.
675

Hijmans, R.J., S.E. Cameron, J.L. Parra, P.G. Jones and A. Jarvis.: [Very high resolution interpolated climate surfaces for global land areas](#). *International Journal of Climatology*, 25(15), 1965-1978, 2005.

Hirata, Y.: The effects of footprint size and sampling density in airborne laser scanning to extract individual trees in mountainous terrain. Proc. ISPRS WG VIII/2 "Laser-scanners for forestry and landscape assessment", Vol. XXXVI, Part 8/W2, 3-6 October 2004, Freiburg, Germany, 2004.

Hopkinson, C.: The influence of flying altitude, beam divergence, and pulse repetition frequency on laser pulse return intensity and canopy frequency distribution. *Can. J. Remote Sens.*, 33(4), 312-324, 2007.

Hubbell, S. P., Foster, R. B., O'Brien, S. T., Harms, K. E., Condit, R., Wechsler, B., Wright, S. J. and De Lao, S. L.: Light gap disturbances, recruitment limitation, and tree diversity in a neotropical forest. *Science*, 283, 554-557, 1999.

Jubanski, J., Ballhorn, U., Kronseder, K., Franke, J., and Siegert, F.: Detection of large above-ground biomass variability in lowland forest ecosystems by airborne [Lidar](#). *Biogeosciences*, 10(6), 3917-3930, 2013.

Kellner, J. R., and Asner, G. P.: Convergent structural responses of tropical forests to diverse disturbance regimes. *Ecol. Lett.*, 12(9), 887-897, 2009.

Laurance, W. F., Delamônica, P., Laurance, S. G., Vasconcelos, H. L., and Lovejoy, T. E.: Conservation: rainforest fragmentation kills big trees. *Nature*, 404(6780), 836-836. doi:10.1038/35009032, 2000.

Le Toan, T., Quegan, S., Davidson, M. W. J., Balzter, H., Paillou, P., Papathanassiou, K., Plummer, S., Rocca, F., Saatchi, S., Shugart, H. and Ulander, L.: The BIOMASS mission: Mapping global forest biomass to better understand the terrestrial carbon cycle. *Remote Sens. Environ.*, 115(11), 2850-2860, 2011.

Lefsky, M. A., Cohen, W. B., Parker, G. G., and Harding, D. J.: [Lidar](#) remote sensing for ecosystem studies, *BioScience*, 52, 19-30, 2002.

Lefsky, M. A.: A global forest canopy height map from the Moderate Resolution Imaging Spectroradiometer and the Geoscience Laser Altimeter System. *Geophys. Res. Lett.*, 37(15), 2010.

Lefsky, M. A., Keller, M., Pang, Y., De Camargo, P. B., and Hunter, M. O.: Revised method for forest canopy height estimation from Geoscience Laser Altimeter System waveforms. *J. Appl. Remote Sens.*, 1(1), 013537, 2007.

Leitold, V., Keller, M., Morton, D. C., Cook, B. D., and Shimabukuro, Y. E.: Airborne [Lidar](#)-based estimates of tropical forest structure in complex terrain: opportunities and trade-offs for REDD+. *Carbon Balance Management*, 10(1), 3, 2015.

Formatted: Widow/Orphan control, Adjust space between Latin and Asian text, Adjust space between Asian text and numbers

720 Mascaro, J., Detto, M., Asner, G. P., and Muller-Landau, H. C.: Evaluating uncertainty in mapping
721 forest carbon with airborne [Lidar](#). *Remote Sens. Environ.*, 115, 3770-3774, 2011.
722
723 Meyer, V., Saatchi, S. S., Chave, J., Dalling, J. W., Bohlman, S., Fricker, G. A., Robinson, C.,
724 Neumann, M., and Hubbell, S.: Detecting tropical forest biomass dynamics from repeated airborne
725 [Lidar](#) measurements. *Biogeosciences*, 10(8), 5421-5438, 2013.
726
727 Minh, D. H. T., Le Toan, T., Rocca, F., Tebaldini, S., Villard, L., Réjou-Méchain, M., Phillips, O.
728 L., Feldpausch, T.R., Dubois-Fernandez, P., Scipal, K. and Chave, J.: SAR tomography for the
729 retrieval of forest biomass and height: Cross-validation at two tropical forest sites in French
730 Guiana. *Remote Sens. Environ.*, 175, 138-147, 2016.
731
732 Nepstad, D. C., Tohver, I. M., Ray D., Moutinho, P., and Cardinot, G.: Mortality of large trees and
733 lianas following experimental drought in an Amazon forest. *Ecology* 88, 2259–2269, 2007.
734
735 Nogueira, E. M., Fearnside, P. M., Nelson, B. W., and França, M. B.: Wood density in forests of
736 Brazil's 'arc of deforestation': Implications for biomass and flux of carbon from land-use change
737 in Amazonia. *Forest Ecol. and Manag.*, 248(3), 119-135, 2007.
738
739 Packalen, P., Strunk, J. L., Pitkänen, J. A., Temesgen, H., and Maltamo, M.: Edge-tree correction
740 for predicting forest inventory attributes using area-based approach with airborne laser scanning.
741 *IEEE J. Sel. Top. Appl.*, 8(3), 1274-1280, 2015.
742
743 Pascual, M., and Guichard, F.: Criticality and disturbance in spatial ecological systems. *Trends*
744 *Ecol. Evol.*, 20(2), 88-95, 2005.
745
746 Pearson, T. R., Brown, S., and Casarim, F. M.: Carbon emissions from tropical forest degradation
747 caused by logging. *Environ. Res. Lett.*, 9(3), 034017, 2014.
748
749 Phillips, O. L., Malhi, Y., Higuchi, N., Laurance, W. F., Núñez, P. V., Vásquez, R. M., Laurance,
750 S. G., Ferreira, L. V., Stern, M., Brown, S. and Grace, J.: Changes in the carbon balance of tropical
751 forests: evidence from long-term plots. *Science*, 282(5388), 439-442, 1998.
752
753 Phillips, O. L., Aragão, L. E., Lewis, S. L., Fisher, J. B., Lloyd, J., López-González, G., Malhi, Y.,
754 Monteagudo, A., Peacock, J., Quesada, C. A. and Van Der Heijden, G.: Drought sensitivity of the
755 Amazon rainforest. *Science*, 323(5919), 1344-1347, 2009.
756
757 Popescu, S. C., Wynne, R. H., and Nelson, R. F.: Measuring individual tree crown diameter with
758 [Lidar](#) and assessing its influence on estimating forest volume and biomass. *Can. J. Remote Sens.*,
759 29(5), 564-577, 2003.
760
761 [Quesada, C. A., Lloyd, J., Anderson, L. O., Fyllas, N. M., Schwarz, M., and Czimczik, C. I.:](#)
762 [Soils of Amazonia with particular reference to the RAINFOR sites, *Biogeosciences*, 8, 1415-](#)
763 [1440, <https://doi.org/10.5194/bg-8-1415-2011>, 2011.](#)
764
765 R Core Team, 2014. R: A language and environment for statistical computing. R Foundation for

766 Statistical Computing, Vienna, Austria. URL <http://www.R-project.org/>.
767
768 Réjou-Méchain, M., Tymen, B., Blanc, L., Fauset, S., Feldpausch, T. R., Monteagudo, A., Phillips,
769 O. L., Richard, H. and Chave, J.: Using repeated small-footprint [Lidar](#) acquisitions to infer spatial
770 and temporal variations of a high-biomass Neotropical forest. *Remote Sens. Environ.*, 169, 93-
771 101, 2015.
772
773 Rocca, F., Dinh, H. T. M., Le Toan, T., Villard, L., Tebaldini, S., d'Alessandro, M. M., and Scipal,
774 K.: Biomass tomography: A new opportunity to observe the earth forests. *Int. Geosci. Remote*
775 *Se.*, 1421-1424, 2014.
776
777 Saatchi, S. S., Harris, N. L., Brown, S., Lefsky, M., Mitchard, E.T., Salas, W., Zutta, B. R.,
778 Buermann, W., Lewis, S. L., Hagen, S. and Petrova, S.: Benchmark map of forest carbon stocks
779 in tropical regions across three continents. *P. Natl Acad. Sci. USA*, 108(24), 9899-9904, 2011.
780
781 Saatchi, S. S., Asefi-Najafabady, S., Malhi, Y., Aragão, L. E., Anderson, L. O., Myneni, R. B.,
782 and Nemani, R.: Persistent effects of a severe drought on Amazonian forest canopy. *P. Natl Acad.*
783 *Sci. USA*, 110(2), 565-570, 2013.
784
785 Santiago, L. S., Goldstein, G., Meinzer, F. C., Fisher, J. B., Machado, K., Woodruff, D., and Jones,
786 T.: Leaf photosynthetic traits scale with hydraulic conductivity and wood density in Panamanian
787 forest canopy trees. *Oecologia*, 140(4), 543-550, 2004.
788
789 Simard, M., Pinto, N., Fisher, J. B., and Baccini, A.: Mapping forest canopy height globally with
790 spaceborne [lidar](#). *Journal of Geophysical Research - Biogeosciences*, 116, G04021,
791 doi:10.1029/2011JG001708, 2011.
792
793 Slik, J. W., Paoli, G., McGuire, K., Amaral, I., Barroso, J., Bastian, M., Blanc, L., Bongers, F.,
794 Boundja, P., Clark, C. and Collins, M. : Large trees drive forest aboveground biomass variation in
795 moist lowland forests across the tropics. *Global Ecol. and Biogeogr.*, 22(12), 1261-1271, 2013.
796
797 Solé, R. V., and Manrubia, S. C.: Are rainforests self-organized in a critical state?. *J. Theor. Biol.*,
798 173(1), 31-40, 1995.
799
800 Strigul, N., Pristinski, D., Purves, D., Dushoff, J., and Pacala, S.: Scaling from trees to forests:
801 tractable macroscopic equations for forest dynamics. *Ecol. Monogr.*, 78(4), 523-545, 2008.
802
803 Ter Steege, H., Pitman, N. C., Phillips, O. L., Chave, J., Sabatier, D., Duque, A., Molino, J. F.,
804 Prévost, M. F., Spichiger, R., Castellanos, H. and Von Hildebrand, P.: Continental-scale patterns
805 of canopy tree composition and function across Amazonia. *Nature*, 443(7110), 444-447, 2006.
806
807 Ter Steege, H., Pitman, N.C., Sabatier, D., Baraloto, C., Salomão, R. P., Guevara, J.E., Phillips,
808 O. L., Castilho, C. V., Magnusson, W. E., Molino, J. F. and Monteagudo, A. :Hyperdominance in
809 the Amazonian tree flora. *Science*, 342(6156), 1243092, 2013.
810

811 Vauhkonen, J., Ene, L., Gupta, S., Heinzl, J., Holmgren, J., Pitkänen, J., Solberg, S., Wang, Y.,
812 Weinacker, H., Hauglin, K. M. and Lien, V.: Comparative testing of single-tree detection
813 algorithms under different types of forest. *Forestry*, 85(1), 27-40, 2011.
814
815 Vauhkonen, J., Næsset, E., and Gobakken, T.: Deriving airborne laser scanning based
816 computational canopy volume for forest biomass and allometry studies. *ISPRS J. Photogramm.*,
817 96, 57-66, 2014.
818
819 Vincent, G., Sabatier, D., Blanc, L., Chave, J., Weissenbacher, E., Pélissier, R., Fonty, E., Molino,
820 J. F. and Couteron, P.: Accuracy of small footprint airborne **Lidar** in its predictions of tropical
821 moist forest stand structure. *Remote Sens. Environ.*, 125, 23-33, 2012.
822
823 West, G.B., Enquist, B. J. and Brown, J. H. : A general quantitative theory of forest structure and
824 dynamics. *P. Natl Acad. Sci. USA*, 106, 7040–7045, 2009.
825
826 Zhou, J., Proisy, C., Descombes, X., Hedhli, I., Barbier, N., Zerubia, J., Gastellu-Etchegorry, J.
827 P. and Couteron, P.: Tree crown detection in high resolution optical and **Lidar** images of tropical
828 forest. *P. Soc. Photo-Opt. Ins.*, 7824. SPIE, 2010.▼

Deleted: .

... [1]

832
833
834
835
836
837
838
839
840

|

|

841

842

Table 1. Information on forest inventory plots. * Indicates that a site has been used for the calibration of the LCA model. Sources: Antimary and Cotriguaçu: (d'Oliveira et al., 2012; Fearnside, 1997), BCI: Center for Tropical Forest Science (CTFS) (Condit, 1998; Hubbell et al., 1999, 2005), Chocó: (bioredd.org), La Selva: Carbono project (Clark and Clark, 2000), Manaus and Tapajós: Espírito-Santo (unpublished results), Nouragues: (Réjou-Méchain et al., 2015), Paracou: (Gourlet-Fleury et al., 2004; Vincent et al., 2012). Rainfall data from WorldClim (Hijmans et al., 2005). AGB: aboveground biomass, WD: wood density.

Site	Data	Plots Size (ha)	N plots	Year	Mean WD (g cm ⁻³)	Mean AGB (Mg ha ⁻¹)	Annual rainfall (mm)
Antimary (Brazil)	Plot level	0.25	50	2010	0.61	234	2000
BCI * (Panama)	Tree level	1	50	2010	0.56	235	2600
Chocó (Colombia)	Tree level	0.25	42	2013	0.60	224	6000
Cotriguaçu (Brazil)	Not available	-	-	-	0.60	-	2000
La Selva * (Costa Rica)	Tree level	1	11	2009	0.45	178	4000
Manaus (Brazil)	Tree level	0.25	10	2014	0.66	263	2200
Nouragues * (French Guiana)	Plot level	1	33	2012	0.66	424	3000
	Tree level	1	7/33				
Paracou * (French Guiana)	Plot level	1	85	2009-10	0.71	353	3000
Tapajós (Brazil)	Tree level	0.25	10	2014	0.62	238	1900

|

Deleted: i
Deleted: ; d'Oliveira et al., 2012

Deleted: :
Formatted: Font:10 pt
Deleted: yr⁻¹

Deleted: 10

848 **Table 2.** Information on **Lidar** data and locations of the 9 research sites.

Site	Sensor	Year	Retur	Flight	Scanning	Frequency	NW corner lat	NW corner lon
(1km ² images)			ns m ⁻²	Altitude (m)	angle (°)	(kHz)		
Antimary	Optech ALTM3100EA	2010-2011	10-15	500	11	70	9°17'47.26"S	68°17'15.06"W
BCI	Optech ALTM3100EA	2009	8	1000	35	70	9°9'28.56"N	79°51'18.9"W
Chocó	Optech ALTM3033	2013	4	1000	20	33	3°57'5.71"N	76°49'10.31"W
Cotriguaçu	Optech ALTM3100EA	2011	10-15	850	11	60	9°27'8.87"S	58°51'51.22"W
La Selva	Optech ALTM3100EA	2009	4	1500	20	70	10°25'37.97"N	84°1'8.76"W
Manaus	Optech ALTM3100EA	2012	10-15	850 (max)	11	60	2°56'38.48"S	59°56'12.57"W
Nouragues	Riegl LMS-Q560	2012	12	400	45	200	4°3'10.0"N	52°42'19.95"W
Paracou	Riegl LMS-280i	2009	4	120-220	30	24	5°15'47.73"N	52°56'26.96"W
Tapajós	Optech ALTM3100EA	2011	10-15	850 (max)	11	60	2°50'53.41"S	54°57'44.53"W

849

850

|

851 **Table 3.** Coefficients, R^2 , RMSE and bias for the models used to estimate AGB_{LCA} without and with wood density
 852 (WD) as a weighting factor (m_{LCA}) and m_{LCA_wd} , respectively).

Model	Equation	a	b	R^2	RMSE	Bias	R^2 cross-val	RMSE cross-val	Bias cross-val
m_{LCA}	$AGB = aLCA + b$ (Eq. (2))	3.56	136.91	0.59	62.53	0.0	0.58	63.26	0.16
m_{LCA_wd}	$AGB = (aLCA+b) \times WD$ (Eq. (3))	4.47	270.27	0.78	46.02	-0.76	0.77	46.47	-0.63

853
 854

856 **Figure 1.** Segmentation of the 1 km × 1 km images in each site using five canopy height thresholds. A minimum of
 857 100 contiguous pixels was used as a segmentation threshold in all cases.

858
 859 **Figure 2.** LCA in function of height thresholds in the nine study sites. The steepest slopes are between 24 m
 860 (Antimary) and 30 m (Nouragues), with an average of 27 m across sites. Steepness of slope was obtained by calculating
 861 the derivative of the sigmoid models characterizing each site.

862
 863 **Figure 3.** Distribution of R^2 between tree height thresholds used to determine LCA and AGB_{local} in the nine 1 ha
 864 subareas (a) and distribution of R^2 between tree height thresholds and AGB_{inv} in 1 ha inventory plots of the four
 865 calibration sites (b). All optimal thresholds are between 23 m and 30 m. The average maximal height threshold is 27
 866 m.

867
 868 **Figure 4.** Relationship between AGB_{inv} and LCA (a), AGB_{inv} normalized by averaged wood density (WD) (b), and
 869 AGB_{inv} vs. AGB_{LCA} estimated with LCA wd model (c). The black line represents the 1-to-1 line. Normalizing AGB
 870 by averaged wood density brings the data from different sites closer to a common fit.

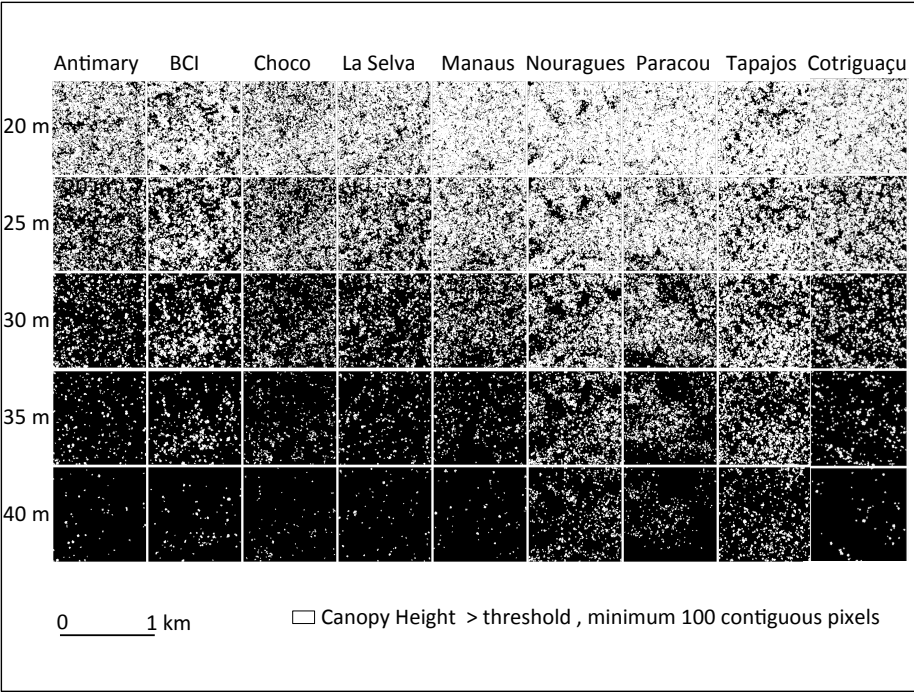
871
 872 **Figure 5.** AGB_{MCH} vs. AGB_{LCA} in the plots of the four calibration sites (a), and AGB_{MCH} vs. AGB_{LCA} in the 1 km²
 873 images of the nine sites (b). The black line represents the 1-to-1 line.

874
 875 **Figure 6.** Detection of changes of forest structure from selective logging in the Antimary study area showing a) the
 876 difference between pre- and post- logging (2010–2011) Lidar derived LCA at 1 ha grid cells over the entire study area,
 877 b) the histogram of LCA for the two Lidar datasets showing the mean difference and the reduction of medium and
 878 large LCA areas from selective logging, c) 2010 Lidar LCA segmentation at 1 m resolution over a sample area in the
 879 north of the study site, d) same LCA segmentation for 2011 Lidar data, and e) difference of the two segmented areas
 880 showing the extent of the logging impact on large trees in addition to natural changes of forest structure from changes
 881 in canopy gaps from tree falls and tree growth.

882
 883 **Figure 7.** Relationship between LCA and AGB_{LCA} (a) and relationship between AGB_{inv} of large trees (> 50 cm DBH)
 884 and total AGB_{inv} (b). In both cases, the intercepts represent the contribution of small trees to total AGB. Note that
 885 Manaus and Nouragues overlap because they have the same mean wood density, as well as Chocó and Cotriguaçu.

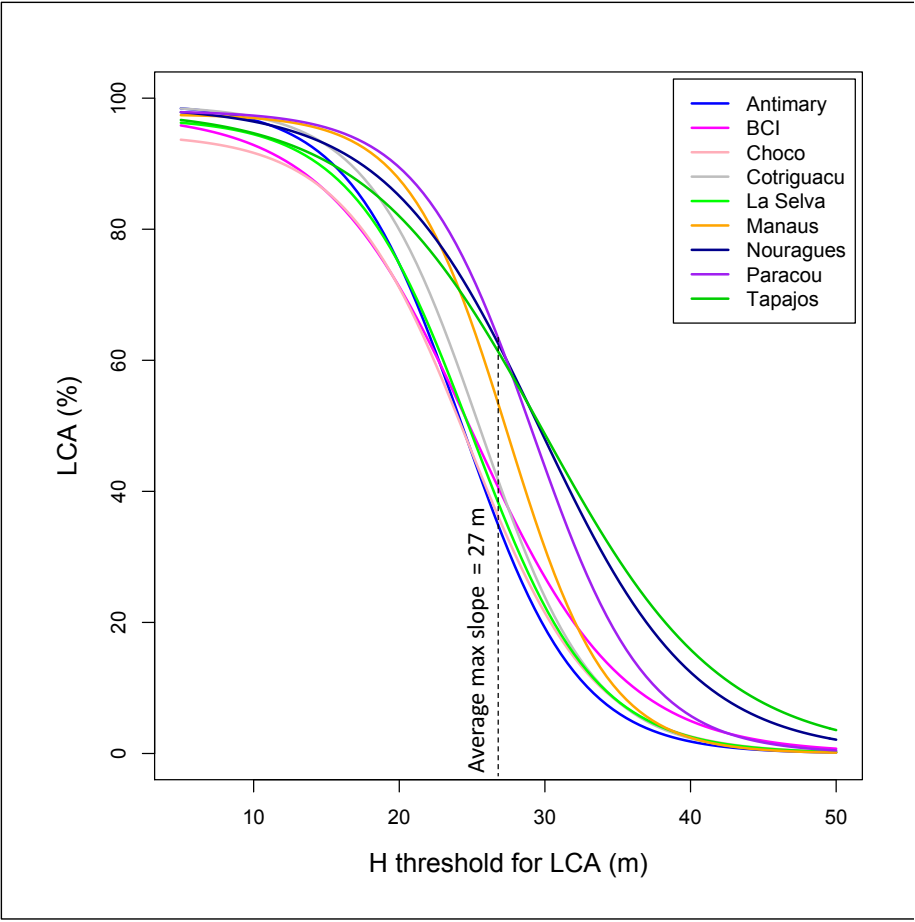
887

888



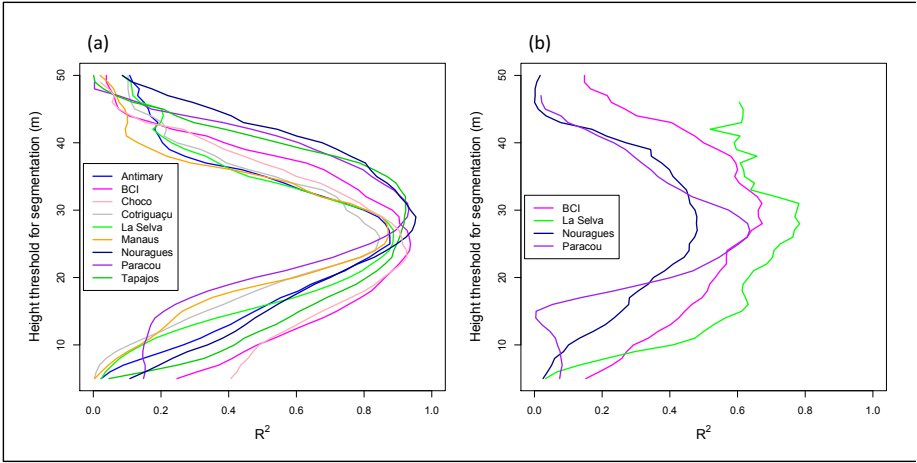
890
891

892 Figure 2

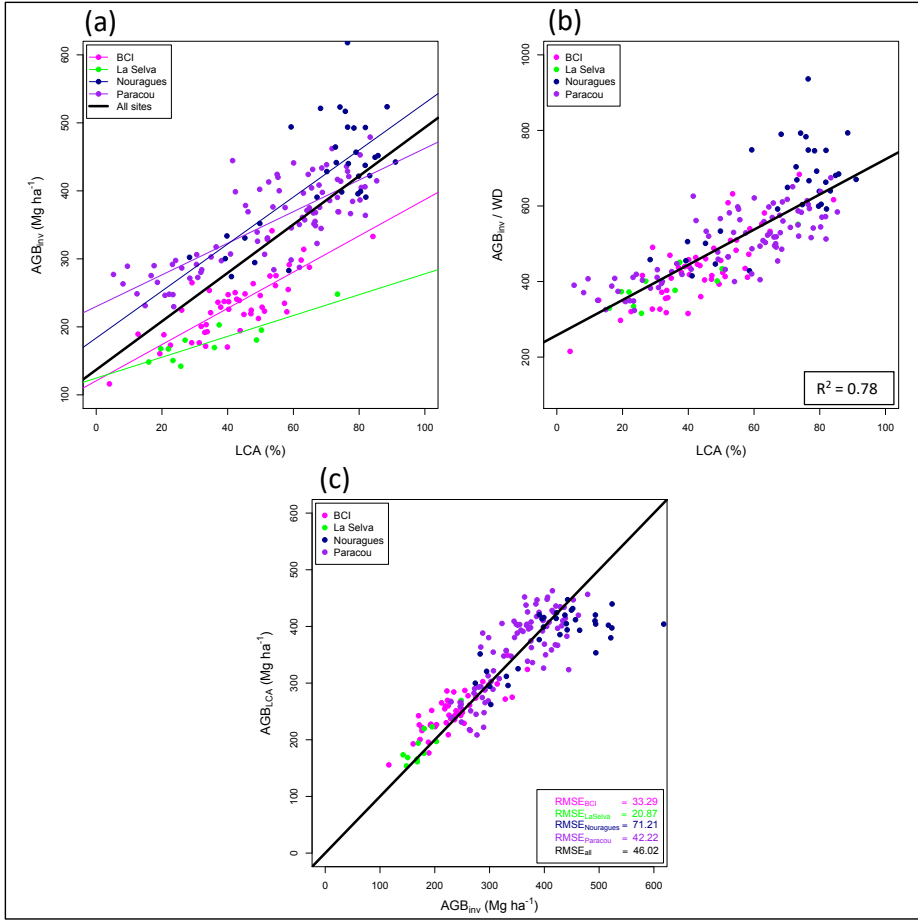


893

894

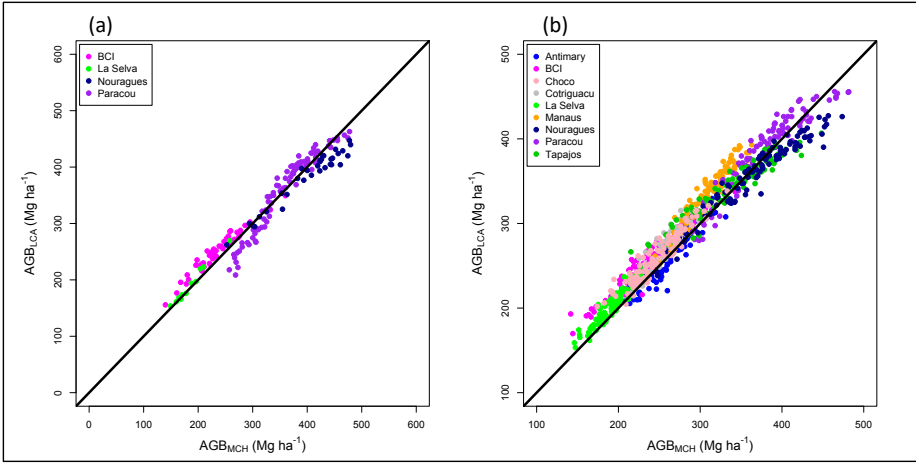


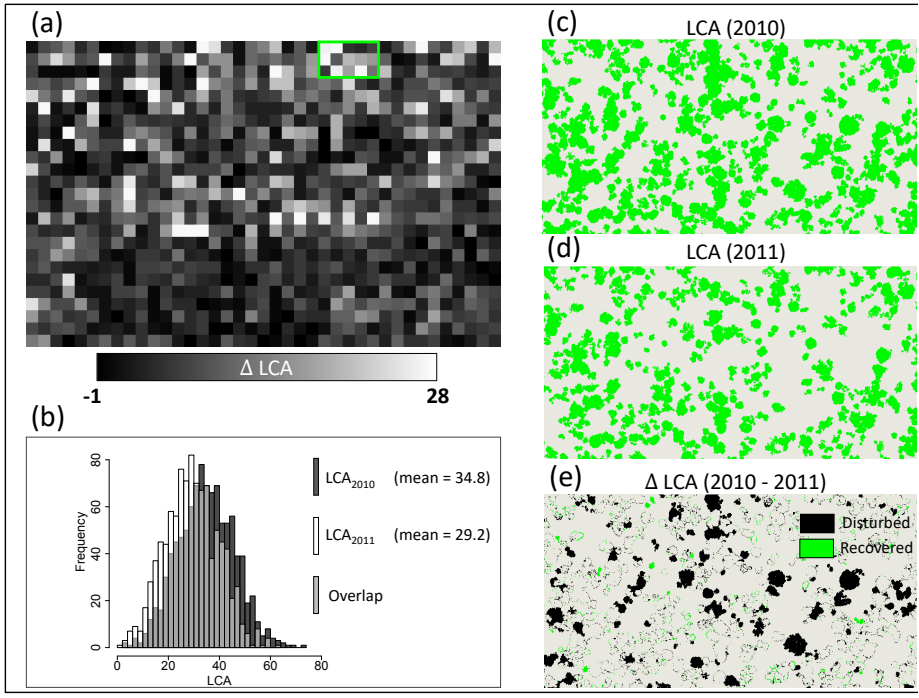
896
897



899
900

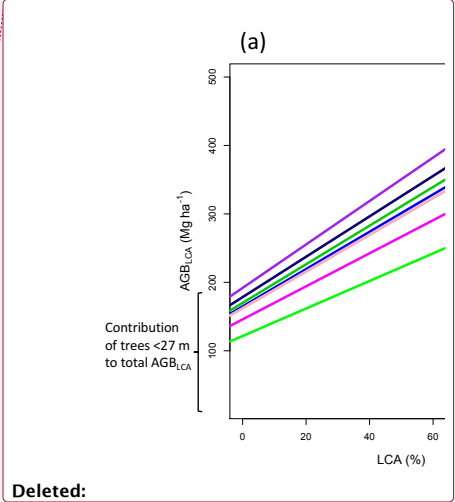
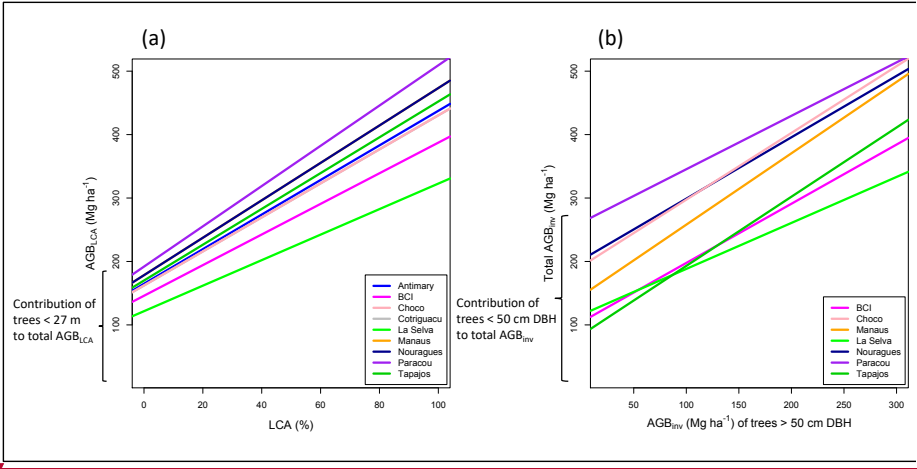
901 Figure 5





906
907

909



, 2010.